Clin Orthop Relat Res (2013) 471:527–536
DOI 10.1007/s11999-012-2562-6

Clinical Orthopaedics and Related Research®
A Publication of The Association of Bone and Joint Surgeons®

SYMPOSIUM: PAPERS PRESENTED AT THE ANNUAL MEETINGS OF THE HIP SOCIETY

# Do Obesity and/or Stripe Wear Increase Ceramic Liner Fracture Risk? An XFEM Analysis

**Jacob M. Elkins MS, Douglas R. Pedersen PhD, John J. Callaghan MD, Thomas D. Brown PhD**

Published online: 25 September 2012


## Abstract

*Background* Hypothesized risk factors for fracture of ceramic liners include impingement, edge-loading, and cup malpositioning. These risk factors are similar to those for generation of stripe wear. However, it is unclear whether the biomechanical conditions contributing to stripe wear generation also increase the risk for ceramic liner fracture

*Questions/purposes* We asked whether (1) head stripe wear propensity; and (2) cup orientation would correlate with alumina liner fracture risk for instances of normal and elevated body weight.

*Methods* An eXtended Finite Element Method (XFEM) model was developed to investigate these mechanisms. Liner fracture risk for 36-mm alumina bearings was studied by simulating two fracture-prone motions: stooping and squatting. Twenty-five distinct cup orientations were considered with variants of both acetabular inclination and anteversion. Four separate body mass indices were considered: normal (25 kg/m$^2$) and three levels of obesity (33, 42, and 50 kg/m$^2$). Material properties were modified to simulate alumina with and without the presence of dispersed microflaws. The model was validated by corroboration with two previously published ceramic liner fracture studies.

*Results* Of 200 XFEM simulations with flaw-free alumina, fracture occurred in eight instances, all of them involving obesity. Each of these occurred with cups in $\leq$ 37° inclination and in 0° anteversion. For 200 corresponding simulations with microflawed alumina, fracture propensity was greatest for cups with higher (edge loading-associated) scraping wear. Fracture risk was greatest for cups with lower inclination (average 42° for fractured cases versus 48° for nonfractured cases) and lower anteversion (9° versus 20°).

*Conclusions* Fracture propensity for 36-mm liners was elevated for cups with decreased anteversion and/or inclination and under conditions of patient obesity.

*Clinical Relevance* Factors causing stripe wear, including obesity and cup malpositioning, also involve increased risk of ceramic liner fracture and merit heightened concern.

The institution of one or more of the authors has received funding from the National Institutes of Health (AR46601 and AR53553) (TDB, JJC), the Veterans Administration (JJC, TDB), and the National Center for Resource Resources (UL1 RR024979) (JME).
One of the authors (JJC) certifies that he has or may receive payments or benefits, in any one year, an amount in excess of $1,000,000, from DePuy Orthopaedics, Inc., Warsaw, IN. One of the authors (TDB) certifies that he has or may receive payments or benefits, in any one year, an amount in excess of $10,000, from Smith and Nephew Orthopedics, Inc (London, UK).
All ICMJE Conflict of Interest Forms for authors and *Clinical Orthopaedics and Related Research* editors and board members are on file with the publication and can be viewed on request.
This work was performed at the University of Iowa, Iowa City, IA, USA.

J. M. Elkins, D. R. Pedersen, J. J. Callaghan, T. D. Brown (✉)
Department of Orthopaedics and Rehabilitation, Orthopaedic Biomechanics Laboratory, University of Iowa,
2181 Westlawn, Iowa City, IA 52242, USA
e-mail: tom-brown@uiowa.edu

J. M. Elkins, D. R. Pedersen, J. J. Callaghan, T. D. Brown
Department of Biomedical Engineering, University of Iowa, Iowa City, IA, USA

J. J. Callaghan
Iowa City Veterans Administration Medical Center, Iowa City, IA, USA

## Introduction

As of 2009, ceramic-on-ceramic (CoC) bearings were estimated to represent 14% of the US market share for

THA [3]. Owing to continued efforts to reduce the incidence of wear-associated osteolysis, especially in younger, heavier, and more physically active patients, and as a result of numerous recent reports of unacceptably high failure rates for some metal-on-metal devices, use of ceramic implants will likely continue to be widespread for the foreseeable future. However, as evidenced by recent reports [1, 18], the rate of catastrophic failure of ceramic liners in recent-generation ceramic liners has ranged between less than 1% [7] up to as high as 3.5% [14]. Given frequencies in this general range, logistically feasible retrospective clinical investigations typically lack sufficient statistical power to provide reliable quantitative information about risk factors.

Although mechanistic information regarding fracture of ceramic liners is currently minimal, component impingement is believed to be a/the principal risk factor [14, 17, 23, 28, 36]. Component malpositioning [13], microseparation leading to edge loading [33], incomplete seating of modular liners [22], and obesity [30] have also been suggested. Interestingly, similar risk factors have been posited to contribute to edge loading-associated stripe wear of the femoral head as well as to the associated squeaking in CoC implants [35, 37, 38]. To date, however, a formal association among edge loading, aberrant bearing noise, and ceramic fracture risk has yet to be established.

Surrogate physical models of liner fracture risk have been previously developed [20], but their cost and complexity preclude performance of extensive parametric analyses. In principle, computational simulations, specifically finite element (FE) models, hold attraction for wider-scope parametric studies. To date, however, performance of classical linear elastic fracture mechanics (LEFM) analysis has been the only available approach for that purpose. LEFM models [11] are logistically challenging, because they require extraordinary computational and analyst effort, because the location of crack nucleation must be known (or assumed) a priori, and because specialized fracture elements must be positioned accordingly. Additionally, simulation of actual fracture propagation involves ad hoc remeshing, which is extremely laborious even in two dimensions and which is intractable for three-dimensional analysis.

A recent FE modeling advancement known as eXtended Finite Element Modeling (XFEM) has enabled a paradigm shift in this area. The breakthrough advantage to XFEM lies in its ability to model fracture initiation and fracture propagation without complicated model remeshing steps (refer to the Appendix: XFEM Background and Model Development). The corresponding reduction of analyst time/labor permits rapid parametric analysis of design and surgical influences on fracture initiation and propagation in THA ceramic liners. Such capability allows systematic investigation of patient-, implant-, and surgery-specific factors that may mitigate fracture propensity.

Toward explaining such potential associations, an XFEM study of ceramic liner fracture was performed to determine whether fracture risk correlated with (1) head stripe wear generation; and (2) cup orientation for both normal-weight and obese patients.

## Materials and Methods

Please refer to the Appendix for additional details regarding model development, corroboration, and validation.

Two separate CoC THA constructs were considered, including 28-mm and 36-mm implants (Fig. 1). For both, the model consisted of CoC THA hardware (third-generation alumina head and liner, CoC stem) and the hip capsule. The 28-mm implant was used for corroboration and validation purposes (Please see the Appendix.). The 36-mm FE/XFEM investigation was undertaken to analyze stripe wear propensity and fracture risk for a contemporary CoC implant. For this series (summarized in Fig. 2), the relationship between fracture and edge-loading-associated (stripe) wear propensity was investigated for variations in implant orientation and in body mass index (BMI). Effects of cup positioning were investigated by considering 25 distinct orientations. Cup inclination was varied between 30° and 60° (radiographic definition [26]) in 7.5° increments. Similarly, acetabular anteversion was varied between 0° and 30°, again in 7.5° increments. The femoral component orientation was held constant at 16.5° of anteversion [29, 40]. Two fracture-prone motion challenges [11] were considered: stooping and Asian-style squatting. These input motions were determined from an inverse dynamics solution of a 47-muscle optimization model [27]. Because obesity has been identified as a risk factor for both liner fracture [30] and for aberrant bearing noise [16, 38], four distinct BMIs were considered: normal (25 kg/m$^2$), moderately obese (33 kg/m$^2$), morbidly obese (42 kg/m$^2$), and superobese (50 kg/m$^2$). The joint contact loads for different BMIs were linearly scaled from the baseline BMI (26.5 kg/m$^2$) of the test subjects.

Because microscopic imperfections (which are ubiquitous in sintered ceramic materials [15, 39]) decrease the tensile stresses otherwise necessary for fracture, material properties of alumina were varied to simulate liners both with and without microflaws.

Two output metrics were of principal interest: occurrence of liner fracture, and volumetric edge loading-associated (stripe) wear at the bearing surface. Volumetric stripe wear was computed using an Archard-based [2] scraping wear algorithm [10], for which a wear coefficient of $3.0 \times 10^{-9}$ mm$^3$ N$^{-1}$m$^{-1}$ (alumina-on-alumina [25]) was used.

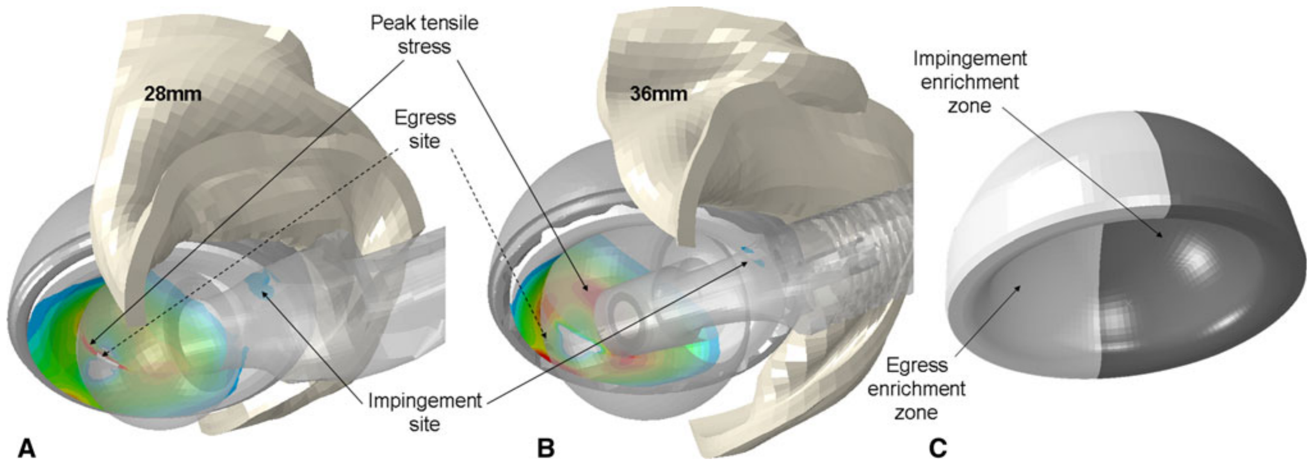


**Fig. 1A–C** The FE model of the global construct consisted of THA hardware and the hip capsule. Two implant geometries were considered: 28-mm (**A**) and 36-mm (**B**) head diameters. Fracture risk was greatest for instances of edge-loading caused by deep flexion with or without the occurrence of component impingement. Fracture initiation occurred as a result of development of tensile stress concentrations that exceeded the material tensile strength. These stress concentrations could occur at two distinct sites: the impingement site (as a result of neck-on-liner contact) and the egress site (resulting from femoral head subluxation and resulting edge-loading). In general, the location of the maximum tensile stress in the 28-mm implant occurred near the cup edge, whereas that for the 36-mm implant was located intermediately between the cup edge and cup pole. Modeling fracture initiation for these locations was enabled by enriching the entire head egress region of the cup (**C**). Additionally, the impingement region was enriched as a separate zone.

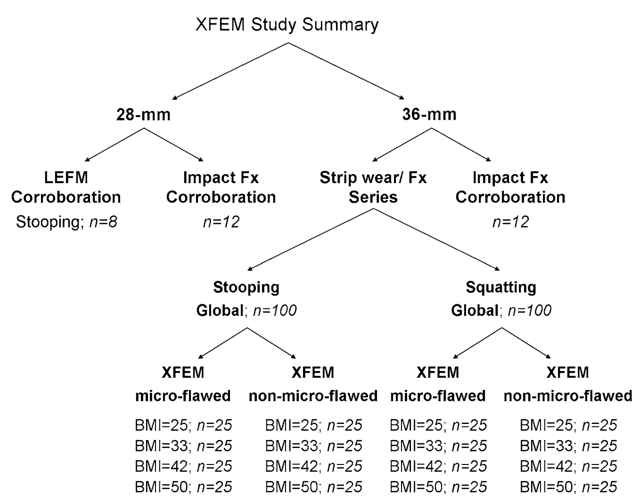


**Fig. 2** Schematic summary of the 632 individual simulations in the study. Both 28- and 36-mm ceramic implants were considered. For the 28-mm liner, two separate model corroboration series were run, including (1) evaluation of the XFEM model against a LEFM fracture model; and (2) corroboration with an physical simulation of ceramic liner fracture (Please refer to the Appendix for further discussion of model corroboration.). For the 36-mm liner, corroboration was also performed for liner impact scenarios. The stripe wear/fracture series consisted of two fracture-prone maneuvers: stooping and squatting. For each of these two motions, 100 total global FE simulations were run: 25 distinct cup orientations times four values of patient BMI. For each global simulation, two additional XFEM analyses were performed simulating both microflawed and nonmicroflawed alumina. (Please refer to the Appendix for additional discussion of model development.) Fx = fracture.

Statistical analyses were performed in Microsoft Excel (Microsoft Inc, Redmond, WA, USA) using the Pearson product-moment correlation for linear regressions.

## Results

Computed femoral head wear stripes/scars were located in similar regions for both squatting and stooping (Fig. 3). Computed volumetric wear from scraping was approximately twice as large for squatting as for stooping. Simulations resulting in fracture, on average, resulted in higher edge loading-associated stripe wear than seen for the nonfractured cases. There was a strong correlation between propensity to fracture (25 component orientations considered for each of four BMI levels) and computed volumetric wear, both for squatting ($r = 0.960$) and for stooping ($r = 0.997$) (Fig. 4).

Fracture risk was dependent on cup orientation (Fig. 5). In general, fracture propensity was greatest for cups in decreased values of inclination and anteversion. The average inclination for liners that fractured was 41.8° versus 47.8° for liners that did not fracture. Average anteversion of fracturing liners was 9.5° compared with 20.1° for nonfracturing cases.

Of the 400 distinct XFEM simulations run, fracture occurred in 108 (Table 1). The majority of fractures initiated in the posterior region of the cup (away from the cup edge) and typically propagated toward the edge (Fig. 6) as head subluxation progressed. The site of fracture initiation corresponded to the approximate location of maximum tensile stress occurring during deep-flexion maneuvers (Fig. 1B). Eight fractures occurred for flaw-free alumina, all involving cases of obesity and cups positioned in 0° anteversion and $\leq 37°$ inclination. One hundred total fractures occurred among the 200 simulations of microflawed alumina. In the normal-weight group, there were

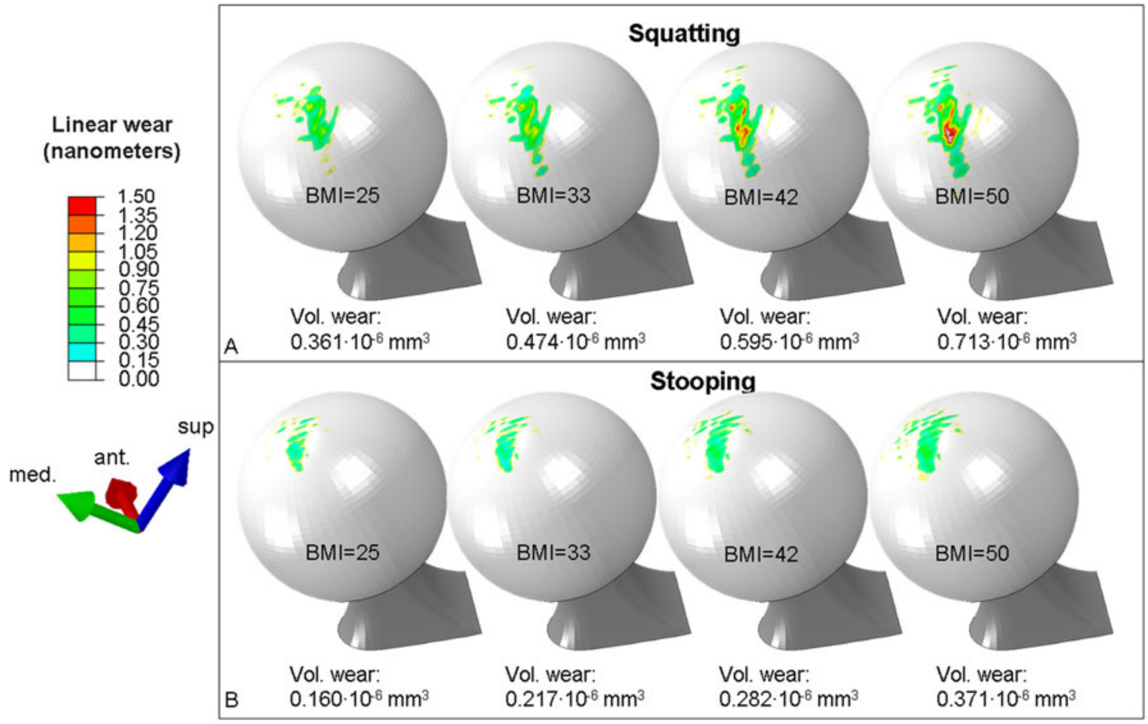


**Fig. 3A–B** The location of edge-loading-associated scraping (stripe) wear generation was similar for the squatting (**A**) and stooping (**B**) simulations. Linear wear depth and total volumetric wear were substantially increased for increased BMI. Computed volumetric wear for squatting was approximately double that for stooping.

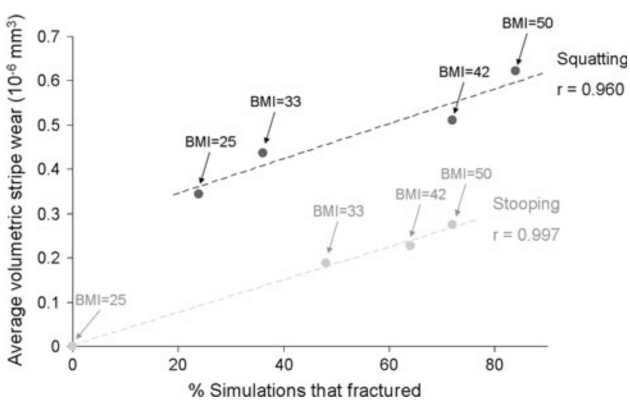


**Fig. 4** Fracture risk correlated with edge-loading-associated volumetric stripe wear computed for both squatting and stooping.

only six fractures (12%), all of which occurred during squatting. However, fracture propensity increased substantially with increased BMI. For the moderately obese group, 21 (42% prevalence) fractures were encountered, of which nine occurred during squatting and 12 during stooping. For the morbidly obese group, there were 34 (68% prevalence) fractures (18 while squatting, 16 while stooping). Thirty-nine (78% prevalence) fractures were observed in the superobese group (21 during squatting, 18 during stooping).

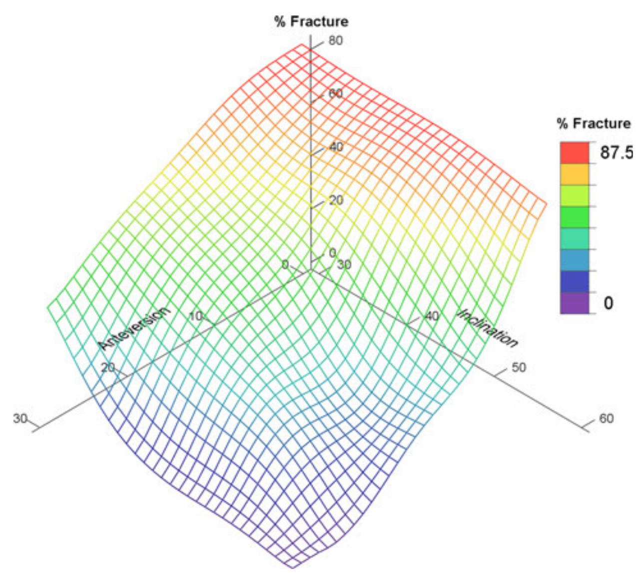


**Fig. 5** Cup orientation dependence of fractures encountered for all 200 simulations of microflawed alumina liners. Increased fracture risk was found for liners oriented in decreased anteversion and/or decreased inclination. For cups positioned in 30° of inclination and 0° of anteversion, 87.5% (seven of eight) of the cases resulted in fracture.

## Discussion

Owing to the increased need for bearing couples suitable for meeting the heightened biomechanical demands from

**Table 1.** Summary of fracture occurrence

| Maneuver | Fracture occurrences | | | | | | | |
|---|---|---|---|---|---|---|---|---|
| | BMI = 25 kg/m$^2$ | | BMI = 33 kg/m$^2$ | | BMI = 42 kg/m$^2$ | | BMI = 50 kg/m$^2$ | |
| | Flaw-free (n = 50) | Microflaws (n = 50) | Flaw-free (n = 50) | Microflaws (n = 50) | Flaw-free (n = 50) | Microflaws (n = 50) | Flaw-free (n = 50) | Microflaws (n = 50) |
| Squatting | 0 | 6 | 2 | 9 | 2 | 18 | 2 | 21 |
| Stooping | 0 | 0 | 0 | 12 | 1 | 16 | 1 | 18 |

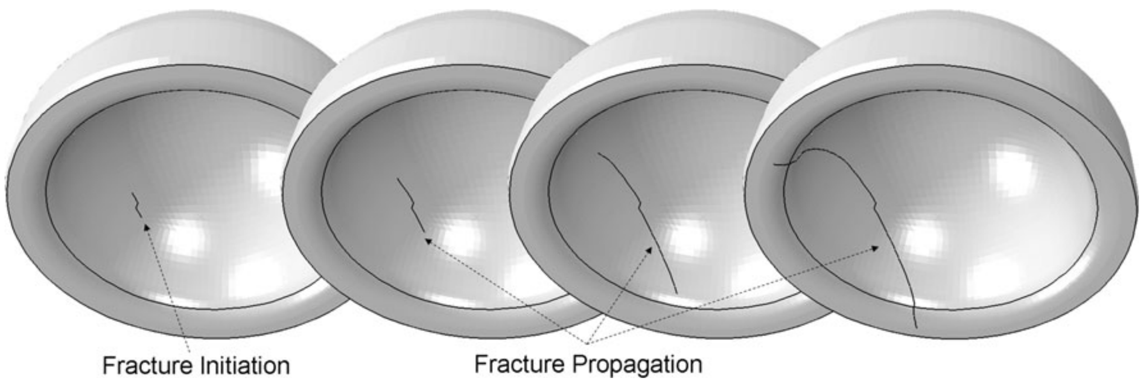


**Fig. 6** For the 36-mm cups, the crack typically initiated distinctly away from the cup edge and then propagated bidirectionally toward the edge as edge-loading progressively increased with further head subluxation.

younger, heavier, and more active patients, ceramic use has rapidly increased in the past decade. Additionally, the recent tissue reactivity problems associated with metal-on-metal implants may plausibly push demand for ceramics even higher. Certainly, advances in materials science and in manufacturing processes have greatly enhanced long-term performance of ceramic bearings. Nevertheless, fracture remains a substantial concern, at least for liners. Catastrophic failure of a ceramic THA holds devastating consequences for the patient, not the least of which is the increased potential for third-body wear of the revision implant as a result of residual ceramic fragments [21]. Recently, the reported prevalence of liner fracture in CoC bearings has been in the range of less than 1% to greater than 2% [1, 7, 14]. Given the potential for increased burden of morbidity resulting from increasing use of CoC bearing couples in mechanically demanding patients, heightened scrutiny is warranted regarding causation of these catastrophic events. Using physical experimentation to study liner fracture is logistically burdensome both in terms of specimen consumption and researcher time. Computational simulation offers an attractive alternative but, unlike for the more commonly studied modes of failure in THA, involves extraordinarily difficulties technically. Conventional (LEFM) fracture analysis requires a priori knowledge of the location of crack nucleation, and it requires specialized meshes and complex postprocessing routines. Moreover, LEFM analysis of fracture propagation in three dimensions—to address realistic clinical circumstances—is prohibitively laborious. However, important questions relating to the biomechanics of ceramic fracture—specifically the influence of obesity and the role of suboptimally positioned components—remain unanswered. The use of XFEM to address these questions has enabled a paradigm shift in this area.

Despite the exciting capabilities that XFEM offers, several simplifications and limitations merit mention. First, the total percentage of simulations resulting in liner fracture in the present study was of course unrepresentatively much higher than that seen clinically. The vast majority of the fractures simulated in this investigation occurred for microflawed alumina, in which subcritical microfractures were assumed to be homogenously dispersed throughout the entire liner. Although microscopic imperfections are ubiquitous in modern ceramics [15, 39], the probability of such an imperfection being just below critical size and existing precisely at the location of greatest tensile stress (as simulated in the present study) is certainly rather low. As a related matter, the size of a given microflaw will determine the degree of associated reduction of the material's mechanical properties. The assumed microflaws posited in the present study represent a mechanical decrement approaching alumina's limiting (initial) stress

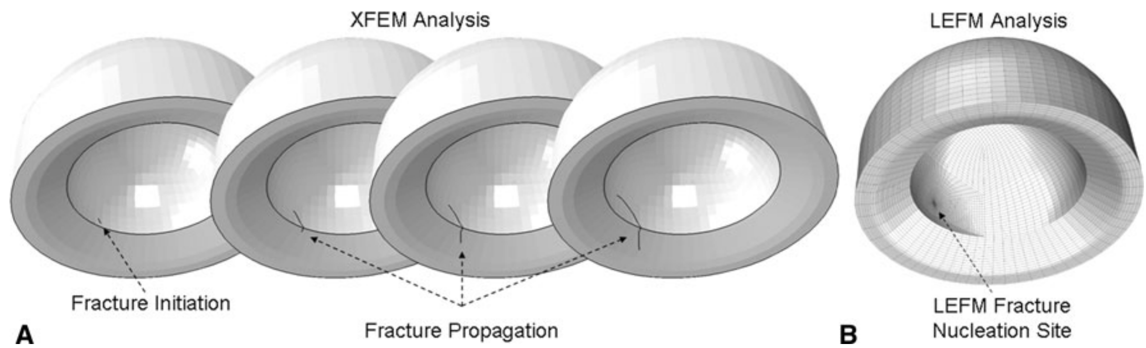


**Fig. 7A–B** (**A**) In contrast to the 36-mm cups (Fig. 6), in cases where fractures occurred for the 28-mm implant, fractures initiated always at the cup edge after impingement and subsequent edge-loading. As the femoral component continued further in flexion, edge-loading severity increased, leading to the crack then propagating away from the cup edge. The location of fracture initiation was similar to that determined from LEFM fracture analysis of an identical bearing (**B**) [11].

intensity factor, $K_{I0}$ [39]. Proof-testing of ceramic implants was initiated to identify the presence of such microflaws immediately after manufacture; therefore, the likelihood is low of implanting a ceramic liner with a microflaw of similar magnitude as represented in the present study. However, the state-space sampling strategy and material property assumptions adopted for the present study design were oriented toward identifying cause-and-effect parametric relationships rather than replicating population-wide experience. (If the great majority of patients undergoing CoC THA were extremely obese individuals with impingement-prone cup orientations and with proclivity for Asian-style squatting, the prevalence of liner fractures would probably be much higher.) Second, we investigated only third-generation (BIOLOX® Forte) alumina ceramic bearings. Although newer, commercially available fourth-generation alumina-composite ceramic demonstrates improved mechanical performance compared with third-generation alumina, the lack of prior experimental or computational data related to fourth-generation fracture characteristics would have hindered model corroboration/validation efforts and therefore precluded use of fourth-generation material properties in this study. Third, stripe wear generation as modeled in the present study did not include the effect of superior rim-loading ensuing from gait-associated bearing microseparation. Although microseparation is a commonly reported mechanism leading to edge-loading and accelerated wear in metal-on-metal bearings [19], the mechanism responsible for stripe wear formation in ceramic bearings is not as clear. Clinical retrievals [37] have suggested the majority of wear stripes do not occur from gait, but instead from posterior edge-loading associated with deep hip flexion, similar to the mechanism of stripe wear posited in the present study. Finally, this investigation involved only two fracture-prone maneuvers. Although stooping and squatting have been previously observed [11] to represent among the greatest challenges to ceramic liner integrity, a seemingly limitless variety of impingement challenges obviously occurs in patient populations. Extension of the present XFEM formulation to investigate additional fracture-prone patient activity maneuvers is an inviting topic for further research.

For the two distinct ceramic liner geometries (28 mm versus 36 mm), both the causative factors for liner fracture propensity and the individual fracture characteristics differed. The 28-mm liners fractured only at the head egress site with fracture initiation occurring very near the cup edge (Fig. 7A). Fracture risk in this group increased with increased cup inclination (Appendix Fig. A3), similar to the behavior simulated using LEFM [11]. (Additionally, earlier LEFM work had identified increased fracture risk with increased anteversion.) Because increased cup inclination and increased anteversion generally protect against neck-on-liner impingement, fracture risk in the 28-mm implant was not strongly correlated with component impingement per se. These findings stand very much in contrast to the fracture characteristics of the 36-mm implant, in which the vast majority of fractures initiated at a location intermediate between the cup edge and cup pole (Fig. 6). Additionally, fracture risk in the 36-mm implant was strongly correlated with component positions that favored impingement (ie, decreased inclination and decreased anteversion).

The percentage of simulations resulting in fracture increased dramatically when BMI was increased from 25 $kg/m^2$ (normal weight) to 33 $kg/m^2$ (moderately obese) and beyond for both flaw-free and microflawed alumina properties. Given the increased intraoperative challenge of component positioning [31] as well as the increased risk of malpositioning [6] with obese patients, the current data suggest that meticulous positioning of CoC THA implants is even more important for obese patients than for those of normal weight. Finally, the present data suggest that edge-loading-associated stripe wear and fracture risk exhibit much more than simply chance association. Because edge-loading and stripe wear have been linked to squeaking in ceramic THAs [35, 37, 38], the present results suggest that squeaking may possibly herald potential catastrophic fracture of the liner. Although the association between squeaking and fracture has been remarked on in the laboratory simulator setting [34], to the authors' knowledge, a formal relationship has not yet been documented clinically. Hopefully the present study may help stimulate increasing vigilance in that regard.

Clearly, XFEM opens exciting new vistas for systematic biomechanical study of ceramic liner fracture. This computational formulation seems especially fertile for application in a design optimization context. Although XFEM has been preliminarily applied to the study of native bone fracture [5], to the authors' knowledge, the present work represents the first application of XFEM to orthopaedic implants.

In summary, an advanced computational platform, XFEM, was used for systematic analysis of ceramic-bearing fracture in THA. The parametric study corroborated recent clinical observations of increased risk of ceramic liner fracture for obese patients. A strong association was identified between scraping/stripe wear severity and fracture risk for instances of both normal and elevated body weight. For both obese and normal-weight simulations, fracture risk was substantially higher for 36-mm cups with decreased anteversion.

**Acknowledgments** Dr Cheryl Liu and the SIMULIA/Abaqus technical support team provided invaluable engineering collaboration during initial development of the XFEM model.

## Appendix

XFEM background and model development

### The eXtended Finite Element Method

The eXtended Finite Element Method (XFEM, also known as the partition of unity method [24]) involves numerical enrichment of a model's geometry so as to allow for solution of the governing differential equations in regions of physical discontinuity such as across fracture surfaces. The XFEM formulation was initially introduced in 1999 to address shortcomings associated with conventional FE treatment of physical discontinuities, especially material cracks [24]. When XFEM is used for fracture analysis, standard displacement fields are enriched near a crack tip by including both discontinuous fields and crack-tip asymptotic fields (Fig. A1).

### Development of the FE/XFEM Fracture Model

The determination of femoral head stripe wear magnitude and ceramic liner fracture propensity involved a multistep approach, previously described [11]. Stresses developed during hip articulation (with or without the occurrence of component impingement) were determined from a global dynamic FE model of THA mechanics. These stresses were then subsequently passed to a separate XFEM submodel of the liner, allowing for fracture initiation and propagation to be simulated. A previously developed and physically validated [12] FE model of the overall THA construct was used for the global analysis. The computational zoning for the global model had been optimized for bearing contact and edge-loading [9] and had been validated by comparison with a corresponding Hertzian analytical contact stress solution reported by Sanders and Brannon [32].

For all global analyses, physical properties of third-generation alumina were used. The liner and head were modeled as linearly elastic (elastic modulus = 380 GPa, Poisson's ratio = 0.23, density = 3.98 gm/cm$^3$) with radial clearance of 0.034 mm and a friction coefficient of 0.04 [4]. Each of these 200 global FE simulations was executed using Abaqus/Explicit (Version 6.10; Dassault Systèmes Simulia Corp, Providence, RI, USA).

Stresses obtained from the global solutions of the Abaqus/Explicit analyses of THA impingement/subluxation were then passed as boundary conditions to the (described previously) (implicit) XFEM submodels. Whereas LEFM analysis would have required extensive ad hoc meshing to reflect the discontinuous material behavior at the initial fracture location [24], the XFEM models were simply partitioned into two distinct so-called "enrichment zones" (see Fig. 1C). For each such enrichment zone, XFEM allows one but only one crack to initiate and propagate within that zone. For the ceramic liner analyses, one enrichment zone was set to correspond to the egress region of the cup, ie, the region associated with head subluxation and edge-loading stress concentrations; the second enrichment zone was that associated with the neck-on-cup impingement region.

Liners without microflaws were modeled as having a damage initiation criterion (flexural strength) of 580 MPa (of maximum principal stress), whereas the flexural strength of alumina with microflaws was taken to be 150 MPa [8]. For both material variants, mixed-mode (tension/in-plane shear/out-of-plane shear) fracture was used with the strain energy release rate (ie, the change in

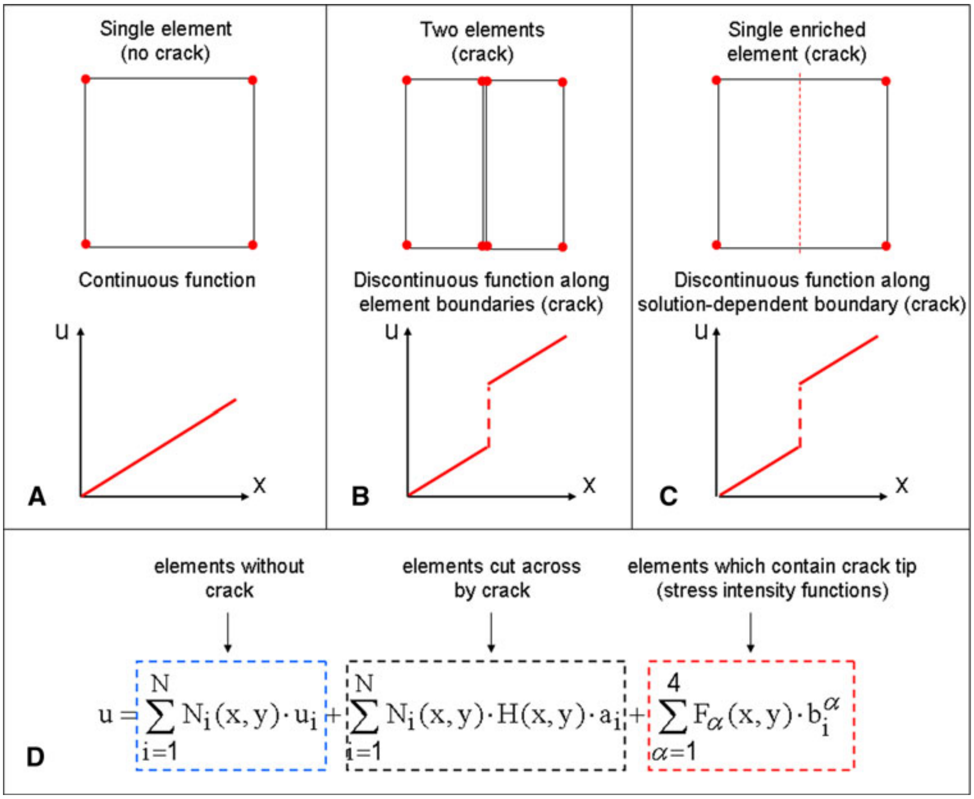


**Fig. A1A–D** Schematic of the XFEM numerical formulation. In standard FE modeling (**A**), the displacement field must be a continuous function across any given element. To model a discontinuity within a given solid object (**B**), a conventional mesh must be structured such that the discontinuity lies across the element boundaries. However, XFEM (**C**) allows for mesh-independent modeling of discontinuities by incorporating enrichment features to augment the standard FE displacement approximation. Element enrichment functions (**D**) allow for discontinuities to exist within a given element, and they allow for approximating stress singularities (unboundedly accentuated local stress concentrations) in the near neighborhood of crack tips. In these mathematical expressions, $u_i$ is the usual nodal displacement vector, $N_i(x,y)$ represents the usual nodal shape functions, $a_i$ and $b_i$ are enriched degree-of-freedom vectors, $H(x,y)$ is the Heaviside step function, and $F_\alpha(x,y)$ are crack tip functions.

potential energy per unit change of crack surface area) taken as 42 J/m$^2$ (flaw-free) or 2.6 J/m$^2$ (with microflaws) [39]. The resulting 400 distinct XFEM submodels were then executed using Abaqus/Standard.

## Model Corroboration

Corroboration of the XFEM model was conducted using two separate series. For the first series, correspondence between the XFEM model and a traditional LEFM fracture mechanics formulation [11] was demonstrated for 28-mm alumina bearings. For this series, inclination was varied between 30° and 60° for cups in 10° of anteversion. Fracture propensity was investigated using a stooping fracture challenge, applying otherwise identical loading and boundary conditions as those for the LEFM study.

The second corroboration series, by contrast involving direct experimental comparisons, investigated the neck-on-liner impact force required to induce fracture in ceramic liners. For both the 36- and 28-mm liners (Fig. A2), the habitual site of neck-on-liner impingement was determined from a global analysis of the stooping maneuver for cups positioned in 45° inclination and 0° anteversion. Then, to approximate a previously reported experimental liner fracture series [20], the femoral neck was displaced toward that impingement site along an axis formed between the center of the neck and the impingement site. For each liner geometry, several simulations were performed in which the displacement of the neck was varied relative to the liner. The resulting impact forces varied between 12 and 30 kN. Impact forces required to initiate fracture were then compared with experimentally determined values [20].

## Results of Model Corroboration

For the 28-mm LEFM/XFEM corroboration series, fractures initiated always at the site of head egress as a result of impingement-induced edge loading (Fig. 7A), behavior very similar to that determined using the LEFM approach (Fig. 7B). Additionally, fracture risk determined for the

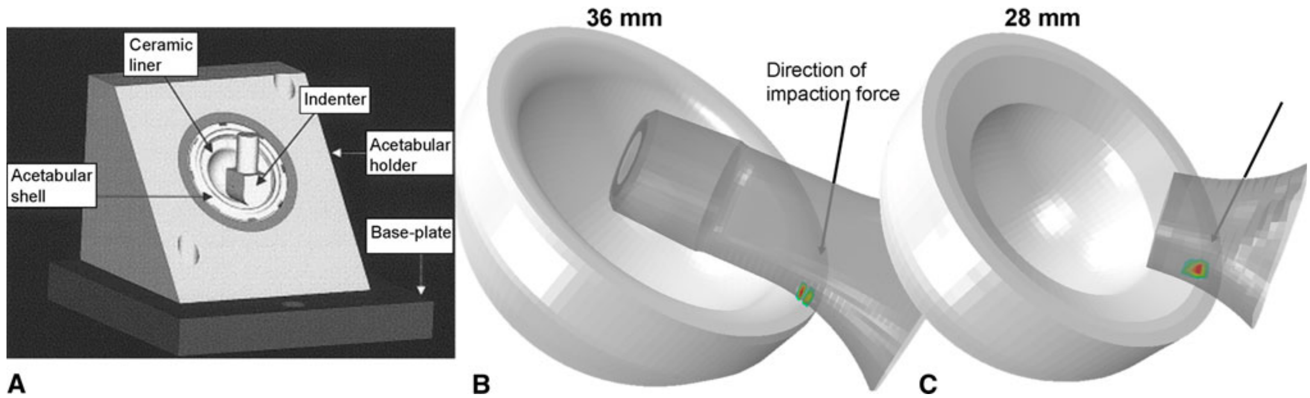


**Fig. A2A–B** An XFEM corroboration series was conducted by computationally replicating the neck-on-liner impact fracture scenario of a previously reported experimental investigation (**A**; reprinted from Maher SA, Lipman JD, Curley LJ, Gilchrist M, Wright TM. Mechanical performance of ceramic acetabular liners under impact conditions. *J Arthroplasty*. 2003;18:936-941, with permission from Elsevier). This corroboration study considered both 36-mm (**B**) and 28-mm (**A**) ceramic liners. Under displacement control, the femoral neck was displaced along an axis passing through the center of the neck and the site of neck-on-liner impingement encountered during a stooping maneuver for cups positioned in 45° inclination and 0° anteversion.

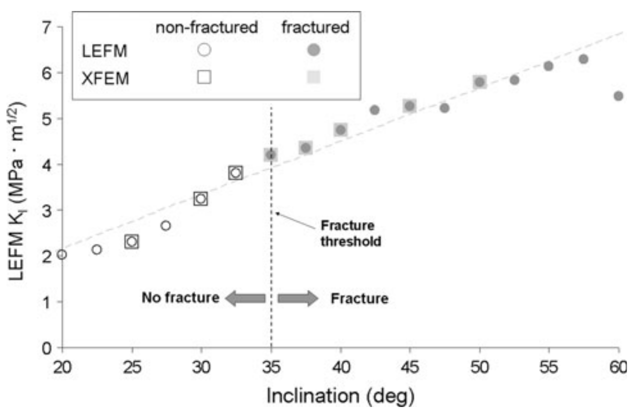


**Fig. A3** LEFM/XFEM corroboration series. XFEM fracture analysis of 28-mm bearings demonstrated similar dependency on cup inclination as that for an LEFM formulation. For both XFEM and LEFM, fracture of the liner occurred for cups positioned in ≥ 35° of inclination for 10° of anteversion. (The criterion for fracture in the LEFM series was that the $K_I$ stress intensity factor exceeded the critical stress intensity factor, $K_{Ic}$.) Data reprinted from Elkins JM, Pedersen DR, Callaghan JJ, Brown TD. Fracture propagation propensity of ceramic liners during impingement-subluxation. *J Arthroplasty*. 2012;27:520-526, with permission from Elsevier.

XFEM formulation increased abruptly for cups abducted greater than a threshold of 35°, a similar threshold to that for abrupt increase of fracture propensity in the LEFM analysis (Fig. A3).

For the neck-on-liner impingement fracture corroboration series, a threshold impaction force of 23.6 kN was computed with cause of fracture for the 28-mm liner (Fig. A4A). A similar fracture threshold force (24.5 kN) was computed for 36-mm liners (Fig. A4B). The corresponding fracture threshold force measured experimentally [20] was 23 kN, lending very strong credence to the credibility of the computational results.

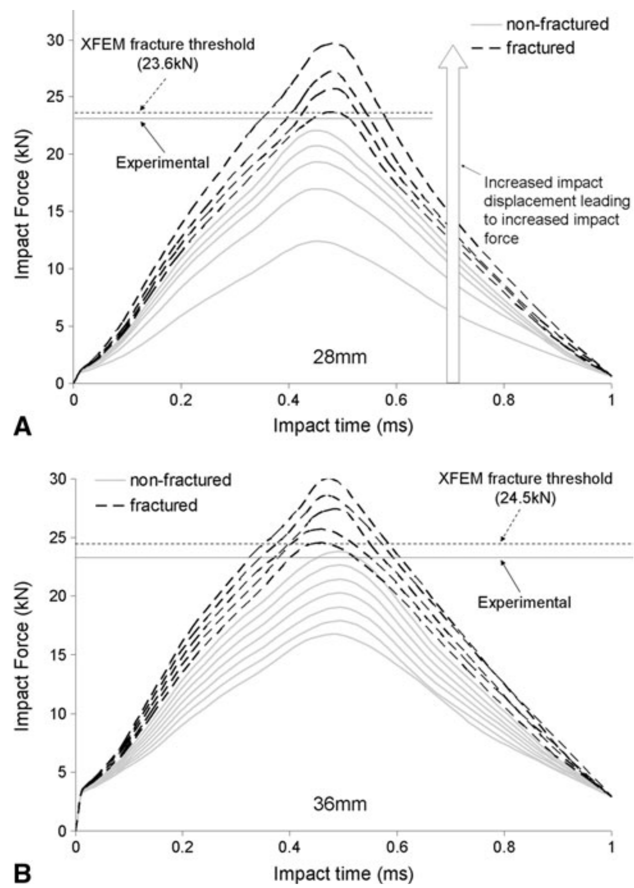


**Fig. A4A–B** Neck-on-liner impact fracture XFEM corroboration from a physical experiment [20]. For both 28-mm (**A**) and 36-mm (**B**) liners, several simulations were run by increasing the amount the neck displacement (leading to increased impact force) into the ceramic liner (see Fig. A2). A fracture threshold contact force of 23.2 kN was determined for 28-mm liners (**A**). A similar threshold force of 24.5 kN was determined for the 36-mm liners (**B**). These compare favorably with an experimentally determined threshold of 23 kN for alumina ceramic liners [20].

## References


1. Amanatullah DF, Landa J, Strauss EJ, Garino JP, Kim SH, Di Cesare PE. Comparison of surgical outcomes and implant wear between ceramic-ceramic and ceramic-polyethylene articulations in total hip arthroplasty. *J Arthroplasty*. 2011;26:72–77.
2. Archard J. Contact and rubbing of flat surfaces. *J Appl Phys*. 1953;24:981–988.
3. Bozic KJ, Kurtz S, Lau E, Ong K, Chiu V, Vail TP, Rubash HE, Berry DJ. The epidemiology of bearing surface usage in total hip arthroplasty in the United States. *J Bone Joint Surg Am*. 2009;91:1614–1620.
4. Brockett C, Williams S, Jin Z, Isaac G, Fisher J. Friction of total hip replacements with different bearings and loading conditions. *J Biomed Mater Res B Appl Biomater*. 2007;81:508–515.
5. Budyn E, Hoc T. Multiple scale modeling of cortical bone fracture in tension using X-FEM. *Eur J Comput Mech v16*. 2007;16:215–238.
6. Callanan MC, Jarrett B, Bragdon CR, Zurakowski D, Rubash HE, Freiberg AA, Malchau H. The John Charnley Award: Risk factors for cup malpositioning: quality improvement through a joint registry at a tertiary hospital. *Clin Orthop Relat Res*. 2011;469:319–329.
7. Capello WN, D'Antonio JA, Feinberg JR, Manley MT, Naughton M. Ceramic-on-ceramic total hip arthroplasty: update. *J Arthroplasty*. 2008;23:39–43.
8. CeramTec AG. *Scientific Information and Performance Data, Biolox Delta—Nanocomposites for Arthroplasty. The Fourth Generation of Ceramics*. Plochingen, Germany: Medical Product Division, CeramTec AG; 2008:11.
9. Elkins JM, Kruger KM, Pedersen DR, Callaghan JJ, Brown TD. Edge-loading severity as a function of cup lip radius in metal-on-metal total hips—a finite element analysis. *J Orthop Res*. 2012;30:169–177.
10. Elkins JM, O'Brien MK, Stroud NJ, Pedersen DR, Callaghan JJ, Brown TD. Hard-on-hard total hip impingement causes extreme contact stress concentrations. *Clin Orthop Relat Res*. 2011;469:454–463.
11. Elkins JM, Pedersen DR, Callaghan JJ, Brown TD. Fracture propagation propensity of ceramic liners during impingement-subluxation. *J Arthroplasty*. 2012;27:520–526.
12. Elkins JM, Stroud NJ, Rudert MJ, Tochigi Y, Pedersen DR, Ellis BJ, Callaghan JJ, Weiss JA, Brown TD. The capsule's contribution to total hip construct stability—a finite element analysis. *J Orthop Res*. 2011;29:1642–1648.
13. Garino JP. Modern ceramic-on-ceramic total hip systems in the United States: early results. *Clin Orthop Relat Res*. 2000;379:41–47.
14. Ha YC, Kim SY, Kim HJ, Yoo JJ, Koo KH. Ceramic liner fracture after cementless alumina-on-alumina total hip arthroplasty. *Clin Orthop Relat Res*. 2007;458:106–110.
15. Hannouche D, Hamadouche M, Nizard R, Bizot P, Meunier A, Sedel L. Ceramics in total hip replacement. *Clin Orthop Relat Res*. 2005;430:62–71.
16. Haq RU, Park KS, Seon JK, Yoon TR. Squeaking after third-generation ceramic-on-ceramic total hip arthroplasty. *J Arthroplasty*. 2012;27:909–915.
17. Hasegawa M, Sudo A, Hirata H, Uchida A. Ceramic acetabular liner fracture in total hip arthroplasty with a ceramic sandwich cup. *J Arthroplasty*. 2003;18:658–661.
18. Lee YK, Yoo JJ, Koo KH, Yoon KS, Kim HJ. Metal neck and liner impingement in ceramic bearing total hip arthroplasty. *J Orthop Res*. 2011;29:218–222.
19. Leslie IJ, Williams S, Isaac G, Ingham E, Fisher J. High cup angle and microseparation increase the wear of hip surface replacements. *Clin Orthop Relat Res*. 2009;467:2259–2265.
20. Maher SA, Lipman JD, Curley LJ, Gilchrist M, Wright TM. Mechanical performance of ceramic acetabular liners under impact conditions. *J Arthroplasty*. 2003;18:936–941.
21. Manley MT, Sutton K. Bearings of the future for total hip arthroplasty. *J Arthroplasty*. 2008;23:47–50.
22. McAuley JP, Dennis DA, Grostefon J, Hamilton WG, Factors affecting modular acetabular ceramic liner insertion: a biomechanical analysis. *Clin Orthop Relat Res*. 2012;470:402–409.
23. Min BW, Song KS, Kang CH, Bae KC, Won YY, Lee KY. Delayed fracture of a ceramic insert with modern ceramic total hip replacement. *J Arthroplasty*. 2007;22:136–139.
24. Moes N, Dolbow J, Belytschko T. A finite element method for crack growth without remeshing. *Int J Numer Meth Engng*. 1999;46:131–150.
25. Morita Y, Nakata K, Ikeuchi K. Wear properties of zirconia/alumina combination for joint prostheses. *Wear*. 2003;254:147–153.
26. Murray D. The definition and measurement of acetabular orientation. *J Bone Joint Surg Br*. 1993;75:228–232.
27. Nadzadi ME, Pedersen DR, Yack HJ, Callaghan JJ, Brown TD. Kinematics, kinetics, and finite element analysis of commonplace maneuvers at risk for total hip dislocation. *J Biomech*. 2003;36:577–591.
28. Park YS, Hwang SK, Choy WS, Kim YS, Moon YW, Lim SJ. Ceramic failure after total hip arthroplasty with an alumina-on-alumina bearing. *J Bone Joint Surg Am*. 2006;88:780–787.
29. Pierchon F, Pasquier G, Cotten A, Fontaine C, Clarisse J, Duquennoy A. Causes of dislocation of total hip arthroplasty. CT study of component alignment. *J Bone Joint Surg Br*. 1994;76:45–48.
30. Poggie RA, Turgeon TR, Coutts RD. Failure analysis of a ceramic bearing acetabular component. *J Bone Joint Surg Am*. 2007;89:367–375.
31. Rittmeister M, Callitsis C. Factors influencing cup orientation in 500 consecutive total hip replacements. *Clin Orthop Relat Res*. 2006;445:192–196.
32. Sanders AP, Brannon RM. Assessment of the applicability of the Hertzian contact theory to edge-loaded prosthetic hip bearings. *J Biomech*. 2011;44:2802–2808.
33. Sariali E, Stewart T, Mamoudy P, Jin Z, Fisher J. Undetected fracture of an alumina ceramic on ceramic hip prosthesis. *J Arthroplasty*. 2010;25:658.e1–685.e5.
34. Stewart TD, Tipper JL, Insley G, Streicher RM, Ingham E, Fisher J. Severe wear and fracture of zirconia heads against alumina inserts in hip simulator studies with microseparation. *J Arthroplasty*. 2003;18:726–734.
35. Taylor S, Manley MT, Sutton K. The role of stripe wear in causing acoustic emissions from alumina ceramic-on-ceramic bearings. *J Arthroplasty*. 2007;22:47–51.
36. Toni A, Traina F, Stea S, Sudanese A, Visentin M, Bordini B, Squarzoni S. Early diagnosis of ceramic liner fracture. Guidelines based on a twelve-year clinical experience. *J Bone Joint Surg Am*. 2006;88(Suppl 4):55–63.
37. Walter WL, Insley GM, Walter WK, Tuke MA. Edge loading in third generation alumina ceramic-on-ceramic bearings: stripe wear. *J Arthroplasty*. 2004;19:402–413.
38. Walter WL, Waters TS, Gillies M, Donohoo S, Kurtz SM, Ranawat AS, Hozack WJ, Tuke MA. Squeaking hips. *J Bone Joint Surg Am*. 2008;90:102–111.
39. Willmann G. Ceramic femoral heads for total hip arthroplasty. *Adv Engng Mater*. 2000;2:114–122.
40. Wines AP, McNicol D. Computed tomography measurement of the accuracy of component version in total hip arthroplasty. *J Arthroplasty*. 2006;21:696–701.